Doped Organic Semiconductors: Trap-Filling, Impurity Saturation, and Reserve Regimes

Max L. Tietze, Paul Pahner, Kathleen Schmidt, Karl Leo,* and Björn Lüssem*

A typical human being carries billions of silicon-based field-effect transistors in his/her pockets. What makes these transistors work is Fermi level control, both by doping and field effect. Organic semiconductors are the core of a novel flexible electronics age, but the key effect of doping is still little understood. Here, precise handling is demonstrated for molar doping ratios as low as 10^{-5} in p- and n-doped organic thin-films by vacuum co-sublimation, allowing comprehensive studying of the Fermi level control over the whole electronic gap of an organic semiconductor. In particular, dopant saturation and reserve regimes are observed for the first time in organic semiconductors. These results will allow for completely new design rules of organic transistors with improved long term stability and precise parameter control.

1. Introduction

Doping is essential for inorganic semiconductor devices in modern CMOS technology, affecting practically every part of our daily lives: communication, mobility, healthcare, etc. Adding small amounts of donor or acceptor type impurities to a semiconductor crystal allows for precise control of the electrical characteristics of the semiconductor, i.e., the charge carrier (type) density and Fermi level position, finally enabling the design of functional electronic devices such as depletion and inversion field effect transistors.[1]

Although molecular doping in organic semiconductors has been studied for a considerable time[2,3] and is applied commercially in displays, it is little understood. In contrast to inorganic semiconductors, particularly the doping efficiency, i.e., the density ratio of generated free charge carriers to dopant molecules, $\eta_{dop} = p/N_A$, is much smaller, sometimes in the range of only a few percent.[4–9] Different approaches have been put forward to explain these low efficiencies, e.g., agglomeration of dopant molecules,[10,11] a large dopant activation energy due to strong coulomb interactions in organic matter,[12] a limitation of doping due to charge traps,[12–14] insufficient energetic disorder caused by neighboring dopant molecules at low concentrations supposed to provide the overcoming of the Coulomb dissociation barrier,[15] and finally hybridization of the dopant and host molecular orbitals.[16]

Here, we propose a new generalized explanation, arguing that the low doping efficiencies are of statistical nature. Compared to inorganic semiconductors, which are supposed to be used in the so-called impurity saturation regime in which all dopants are activated,[1] dopant saturation cannot be reached in organic semiconductors due to the much larger concentrations commonly required in organic electronics.[3] The Fermi level is then located between the dopant level and the transport level, resulting in incomplete activation of dopants known as impurity reserve from classical semiconductor theory. However, for ultralow molar doping ratios in co-evaporated organic thin-films down to $MR \simeq 10^{-5}$, and by using our recently published statistical description of the molecular doping process,[12] we can show that the Fermi level is shifted above a hypothesized dopant level for p-doped layers, i.e., we can access the saturation regime. Almost all dopants are activated and the doping efficiency approaches 100%. In contrast, the dopant reserve is observed at high molar doping ratios. Furthermore, similar n-doping studies on the same host materials give evidence that the saturation regime is achieved there even at high doping concentrations, strongly indicating the presence of very shallow donor states in organic materials.

Highly purified organic semiconductors are indispensable for these studies as impurities and traps usually limit doping at low concentrations.[13,14] Therefore, we chose high-purity pentacene and ZnPc as hosts, each purified threefold by repeated gradient-zone sublimation and p-doped with the acceptors $C_{60}F_{36}$ or F_6-TCNNQ, respectively, or n-doped by the di-metal complex $W_2(hpp)_4$ (cf. **Figure 1**).

Dr. M. L. Tietze,[+] P. Pahner, K. Schmidt,
Prof. K. Leo, Prof. B. Lüssem[++]
Institut für Angewandte Photophysik
Technische Universität Dresden
George-Bähr-Straße 1, 01069 Dresden, Germany
E-mail: max.tietze@iapp.de; leo@iapp.de

[+]Present address: Solar and Photovoltaics Engineering Research Center, King Abdullah University of Science and Technology, 23955–6900 Thuwal, Saudi Arabia

[++]Present address: Department of Physics, Kent State University, Kent, OH 44242, USA

DOI: 10.1002/adfm.201404549

2. Results and Discussion

2.1. UPS on p- and n-Doped Thin-Films

First, pentacene (P5) thin-films p-doped by $C_{60}F_{36}$ or n-doped by $W_2(hpp)_4$ are investigated by ultraviolet photoelectron spectroscopy (UPS). The sample structure reads Ag/MeO-TPD(4 nm)/P5(<65 nm) in which the thin MeO-TPD interlayer

© 2015 WILEY-VCH Verlag GmbH & Co. KGaA, Weinheim

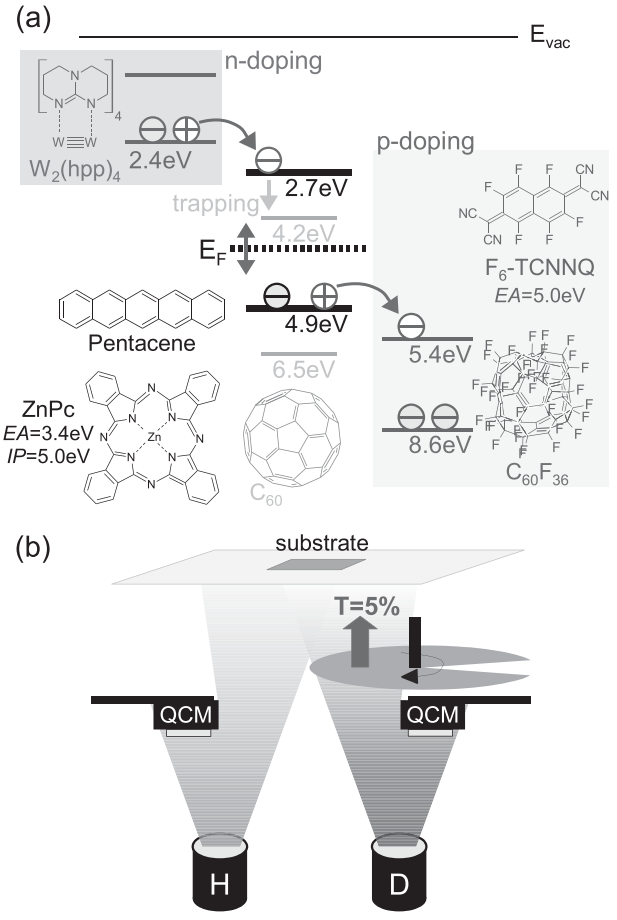

Figure 1. Principle of molecular doping. a) A host material is p-doped (n-doped) by electron transfer from a host (n-dopant) molecule HOMO to an adjacent p-dopant (host) molecule LUMO. The investigated host materials are pentacene (P5) and ZnPc, each n-doped by $W_2(hpp)_4$ or p-doped by $C_{60}F_{36}$ or F_6-TCNNQ. C_{60} molecules constitute electron traps in P5. b) Doped thin-films are processed by vacuum cosublimation employing a rotational shutter for achieving molar doping ratios as low as 10^{-5}.

is introduced to decouple the P5 growth from the underlying metal, i.e., ensuring a reproducible thin-film morphology.

UPS spectra of the doped P5 layers with varying doping concentration are shown in **Figure 2**. With increasing molar doping ratios, a clear shift of the occupied states toward (away) from the Fermi level ($E_B = 0$) is found for p-type (n-type) doping. The determined Fermi level positions with respect to the measured P5 HOMO peaks (indicated by circles in Figure 2) are plotted versus the molar doping ratio in **Figure 3**a for p-doping (n-doping) with downward (upright) triangles. Since the doping ratio covers five orders of magnitude, the whole range from the intrinsic position until saturation is resolved for p-type doping. At doping concentrations below 4×10^{-5}, the Fermi level is found to be pinned close to the intrinsic position ($E_F \approx 1.8$ eV). Doubling the doping ratio to $MR = 8 \times 10^{-5}$ rapidly shifts the Fermi level to 1.29 eV. At medium concentrations, i.e., in the range of $10^{-4} < MR < 10^{-3}$, the Fermi level is shifted by ≈0.4 eV toward the HOMO peak, whereas it moves further by only 0.2 eV at concentrations above 10^{-3} reaching finally $E_F = 0.72$ eV at $MR = 0.33$, which is 0.25 eV above the HOMO onset.

In case of n-doping, such characteristic ranges cannot be identified. Here, there Fermi level position monotonously increases from 2.48 to 2.94 eV within the investigated range of doping concentrations, that is $7 \times 10^{-4} < MR < 0.66$, showing no pronounced kinks. In particular, we found a shift of the Fermi level above the LUMO onset of the P5 host for $MR \geq 0.1$. In contrast, E_F is pinned ≈0.25 eV above the HOMO onset in case of p-type doping. This remarkable difference between p- and n-doping, demonstrated here for the same host material, is in agreement with previous studies, however, there individually performed either on just molecular p-type,[5,9,12] or n-type doping.[13]

2.2. Semiconductor Statistics

It is the purpose of this article to explain the above findings on a fundamental level by application of a statistical description based on classical semiconductor theory. The main assumptions of this approach have been discussed in detail elsewhere,[12] however, the leading ideas/equations are sketched in **Figure 4**a and will be briefly summarized in the following. For a p-doped semiconductor, the neutrality equation reads

$$p + N_T^+ = n + N_A^- \cong N_A^- \tag{1}$$

Here, the hole density p is determined by a Fermi–Dirac integral

$$p = \int_{-\infty}^{\infty} dE\, g_{DOS}(E)\big(1 - f(E, E_F)\big) \tag{2}$$

in which $f(E,E_F)$ is the Fermi–Dirac statistics and $g_{DOS}(E)$ the density-of-states of the host material, typically resembling a superposition of Gaussian and exponential distributions for organic thin-films[12,13,18]

$$g_{DOS}(E) = \begin{cases} \dfrac{N_o}{\sqrt{2\pi}\sigma} \exp\left(-\dfrac{(E-E_o)^2}{2\sigma^2}\right), & E < E_\beta \\ \dfrac{N_\beta}{\beta} \exp\left(-\dfrac{E-E_\beta}{\beta}\right), & E > E_\beta \end{cases} \tag{3}$$

Furthermore, shallow or deep trap states might be present, hindering the doping process in particular at low concentrations. The occupation of these traps is given by an additional Fermi–Dirac integral

$$N_T^+ = \int_{-\infty}^{\infty} dE\, g_T(E)\big(1 - f(E, E_F)\big) \tag{4}$$

in which the trap density $g_T(E)$ is most easily approximated by a single Gaussian

$$g_T(E) = \frac{N_T}{\sqrt{2\pi}\sigma_T} \exp\left(-\frac{(E-E_T)^2}{2\sigma_T^2}\right) \tag{5}$$

However, it could generally resemble any arbitrary shape.[13,20] Finally, dopant ionization is described by activation from a single acceptor level E_A according to

$$N_A^- = \frac{N_A}{1 + \exp\left[(E_A - E_F)/k_B T\right]} \tag{6}$$

© 2015 WILEY-VCH Verlag GmbH & Co. KGaA, Weinheim

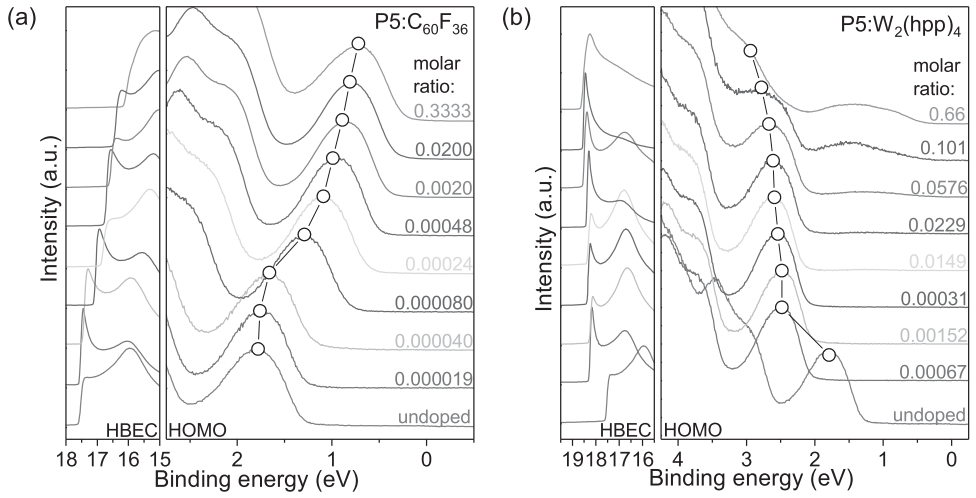

Figure 2. UPS spectra of molecularly doped P5 thin-films. The used sample structure is Ag/MeO-TPD(4 nm)/P5(<65 nm) in which the P5 film is either a) p-doped by $C_{60}F_{36}$ or b) n-doped by $W_2(hpp)_4$.

The depth of E_A with respect to the HOMO center E_0 defines the overall efficiency of the doping process, which is $\eta_{dop} = p/N_A$. In case of highly efficient doping, classically described by shallow dopant states,[1] all dopant molecules are ionized, i.e., $N_A^- = N_A$ and $E_F > E_A$, which is known as impurity saturation. For partial ionization of p-dopants, the Fermi level lies below the acceptor level, which corresponds to a deep impurity level and is called impurity reserve. Thus, for a given dopant level E_A, the transition between impurity saturation and reserve is defined by $E_F = E_A$ and can be achieved either by variation of the temperature at a certain doping concentration,[1,21] or of the doping concentration at fixed temperature as demonstrated here. Numerical solving the neutrality condition (Equation (1)) at a certain temperature (e.g., RT) yields $E_F(MR)$ plots, exhibiting characteristic slopes on a log-scale for trap-limitation, dopant saturation, and reserve as well as corresponding kinks at the transition points between these regimes depending on the specific shapes of the used $g_{DOS}(E)$ and $g_T(E)$ distributions and the depth of the dopant level E_A. Their impact on the shape of $E_F(MR)$ and $\eta_{dop}(MR)$ curves is demonstrated by a detailed parameter study given in the Supporting Information, Figures S1–S4. The main outcomes are strong shifts of the Fermi level at $N_A = N_T$, i.e., at the point of complete trap filling, characteristic kinks at that doping concentration satisfying the transition condition $E_F = E_A$, and a decreasing doping efficiency η_{dop} for higher doping ratios, i.e., for $E_F < E_A$.

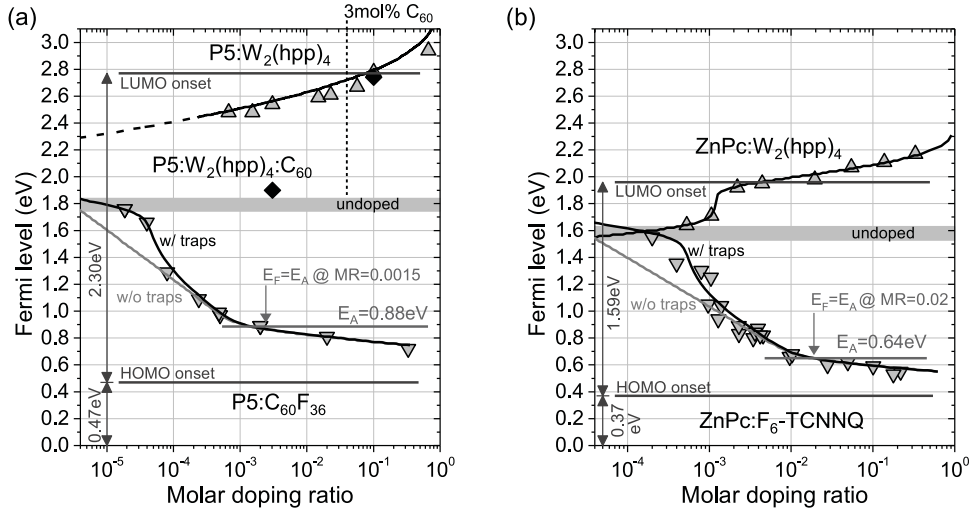

Figure 3. Fermi level versus molar doping ratio: $E_F(MR)$. a) UPS data of pentacene (P5) thin-films p-doped by $C_{60}F_{36}$ (downward triangles) or n-doped by $W_2(hpp)_4$ (upright triangles). The solid lines correspond to respective calculation results applying the statistical description. The transition from dopant saturation to reserve is defined by the condition $E_F = E_A$, appearing at $MR = 0.0015$ for p-type doping. In case of n-type doping, dopant saturation ($N_D^+ = N_D$) has been assumed for all concentrations. Besides, black diamonds indicate the Fermi level position of P5:$W_2(hpp)_4$:C_{60} samples, in which the C_{60} concentration is 3 mol% each. b) Similar UPS and calculation results on ZnPc thin-films, either p-doped by F_6-TCNNQ (downward triangles) or n-doped by $W_2(hpp)_4$ (upright triangles). All Fermi level positions are given with respect to the UPS HOMO peak positions of the host materials. For completeness, the respective HOMO and LUMO onsets determined from UPS/IPES are indicated (see the Supporting Information).[17]

© 2015 WILEY-VCH Verlag GmbH & Co. KGaA, Weinheim

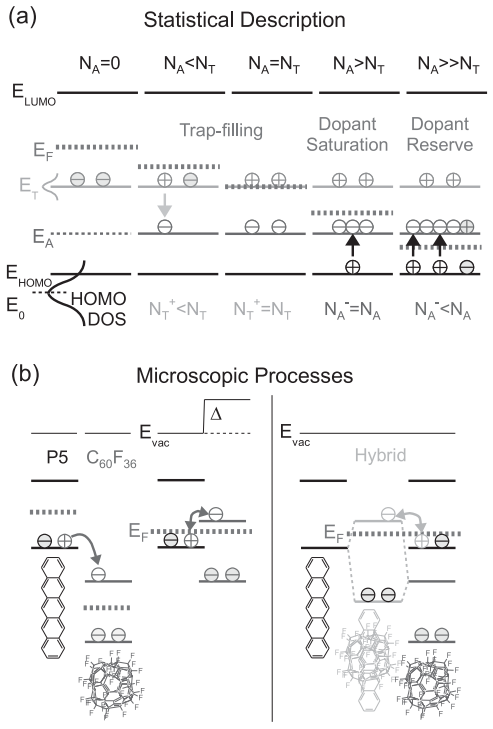

Figure 4. Molecular p-doping models. a) Qualitative illustration of the statistical description. Dopant activation is considered by an effective acceptor level E_A. Trap states E_T hinder the doping process at low concentrations. Free holes are provided by doping for $N_A > N_T$. In this case, either dopant saturation ($N_A^- = N_A$) or reserve ($N_A^- < N_A$) is possible. b) Illustration of the underlying microscopic processes justifying the appearance of E_A. Either direct host-dopant charge transfer (left)[19] or host-dopant hybridization (right)[16] causes dopant related gap states determining the amount of activated dopants in equilibrium.

2.3. Trap-Limitation, Dopant Saturation, and Reserve Regimes in Doped Pentacene, ZnPc, and C_{60} Thin-Films

Comparing the findings from the semiconductor statistics calculations to the measured $E_F(MR)$ UPS data of p-doped P5 films gives evidence for the existence of the trap-limitation, dopant saturation, and reserve regimes. The experimental results can be precisely reproduced by the statistical model over five orders of magnitude (cf. Figure 3a, solid lines), if assuming an acceptor level at $E_A = 0.88$ eV above the HOMO peak and deep hole traps with a density of $N_T = 9.6 \times 10^{16}$ cm^{-3}. The transition between dopant saturation and reserve is seen at $MR \approx 0.0015$, which is even obtained by a calculation without traps (gray line), and the trap-limitation regime is present for $MR < 3.5 \times 10^{-5}$. A fairly equal density of Gaussian distributed hole traps has independently been obtained by impedance spectroscopy on P5:$C_{60}F_{36}$ Schottky diodes, recently published by Pahner et al.[18] Furthermore, they determined doping efficiency values by Mott–Schottky analysis plotted in **Figure 5** in comparison to the calculations provided here. Indeed, Pahner et al. obtained $\eta_{dop} = 0.98$ at $MR = 2 \times 10^{-4}$, which gives strong evidence that dopant saturation is really achieved in this range of doping concentrations. Furthermore, in agreement with the statistical calculations, strongly decreasing doping efficiencies

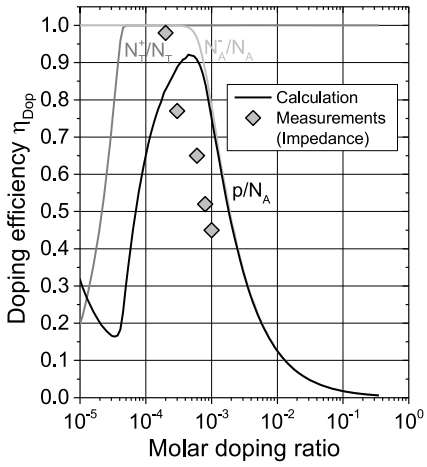

Figure 5. Doping efficiency in P5:$C_{60}F_{36}$ thin-films. Calculated doping efficiency $\eta_{dop} = p/N_A$, fractions of filled traps N_T^+/N_T and ionized dopants N_A^-/N_A for the material system P5:$C_{60}F_{36}$ in comparison the experimental values determined by Mott–Schottky analysis published by Pahner et al.[18]

were measured for higher doping ratios, dropping to $\eta_{dop} = 0.45$ at $MR = 10^{-3}$, clearly indicating the transition to dopant reserve.

In case of P5:W_2(hpp)$_4$, i.e., n-doping of P5, the UPS data can be reproduced by calculating $E_F(MR)$ assuming just dopant saturation for all concentrations, i.e., solving $n = N_D^+ = N_D$. Since here the Fermi level is not pinned by a donor level E_D, it can shift even above the LUMO onset at high concentrations. The curved $E_F(MR)$ correlation is achieved by assuming only a Gaussian LUMO DOS ($E_{0,LUMO} = 3.0$ eV, $\sigma = 0.15$ eV) since an (additional) exponential DOS would result in straight $E_F(MR)$ lines.[22] A limitation by electron traps could not be seen in the range of investigated doping ratios because the Fermi level curve does not show any kink, however, could be present at concentrations below 7×10^{-4}.

Since the LUMO level of C_{60} lies below that of P5 by 1.5 eV (cf. Figure 1), we can instead intentionally introduce deep electron traps by co-evaporation of P5 and C_{60}. These traps can be purposefully filled by n-doping the P5:C_{60} blend with W_2(hpp)$_4$. For validation, two UPS samples with P5:C_{60}:W_2(hpp)$_4$ thin-films are compared: One with $MR(W_2(hpp)_4) < MR(C_{60})$ and the other vice versa. The C_{60} concentration is fixed to $MR \simeq 0.03$, whereas the W_2(hpp)$_4$ concentrations are $MR = 0.003$ and $MR = 0.1$ (black diamonds in Figure 3a). In case of $MR = 0.1$, the Fermi level lies at 2.74 eV which is close to the position without C_{60} ($E_F = 2.78$ eV). For the lightly doped sample, E_F is shifted only to 1.9 eV, i.e., just above the undoped position, whereas $E_F = 2.56$ eV was found for an usual P5:W_2(hpp)$_4$ film. This result clearly confirms that C_{60} molecules act as electron traps in pentacene, which control the Fermi level position at lower doping concentrations. As soon as the n-dopant density exceeds the C_{60} density, all these traps are filled and the Fermi level strongly shifts toward the P5 LUMO. The position of this strong shift is supposed to be tunable by the C_{60} concentration.

To provide broader support for the above conclusions, similar UPS experiments and calculations are performed on ZnPc thin-films either p-doped by the acceptor molecule F_6-TCNNQ or n-doped by W_2(hpp)$_4$. The obtained $E_F(MR)$ correlations are shown in Figure 3b, the associated UPS spectra

© 2015 WILEY-VCH Verlag GmbH & Co. KGaA, Weinheim

are given in the Supporting Information, Figure S5. Similar to P5, trap-limitation, dopant saturation, and reserve regimes can be identified for p-doping as well, if assuming an acceptor level at $E_A = 0.64$ eV defining the transition between impurity saturation and reserve at $MR = 0.02$. Hole traps with a density of $N_T = 7.2 \times 10^{17}$ cm^{-3} hinder efficient p-doping at molar doping ratios below 4.5×10^{-4}, which is in excellent agreement with corresponding conductivity measurements (cf. **Figure 6**). A clear drop of the conductivity by four orders of magnitude is found when varying the doping concentration in-between $10^{-4} < MR < 10^{-3}$, whereas it scales like $\sigma \propto MR^n$ with $n \simeq 1.25$ at higher concentrations, confirming that trap states limit current transport at low concentrations. This finding is further confirmed by conductivity measurements on the system ZnPc:F_4-TCNQ, suggesting the presence of deep hole traps with $MR \approx 3 \times 10^{-4}$ to 6×10^{-4}.[23]

In case of n-doped ZnPc:W_2(hpp)$_4$ films, a shift of the Fermi level above the LUMO onset is found as well, however, appearing already at doping ratios as low as 4×10^{-3}. This behavior can be modeled similarly to n-P5, i.e., by assuming dopant saturation but a much narrower LUMO DOS ($E_{0,\mathrm{LUMO}} = 2.20$ eV, $\sigma = 0.07$ eV). Additionally, electron trap states must be taken into account to reproduce the step in the $E_F(MR)$ plot at $MR \simeq 1.2 \times 10^{-3}$ ($N_T = 1.9 \times 10^{18}$ cm^{-3}).

Finally, n-doped C_{60}:W_2(hpp)$_4$ films are studied by UPS and respective calculations, yielding the same trends as for the n-P5 and n-ZnPc films (cf. Supporting Information, Figure S7). The Fermi level shifts above the LUMO onset in-between $10^{-2} < MR < 10^{-1}$, explained again by dopant saturation. Electron traps control E_F at doping ratios below 2.1×10^{-3} ($N_T = 3.4 \times 10^{18}$ cm^{-3}).

These data are in quantitative agreement with a similar study on the system C_{60}:[RuCp*(mes)]$_2$ published by Olthof et al.,[13] in particular, a Fermi level position of merely 50 meV below the C_{60} LUMO onset at $MR \simeq 0.2$ has been measured. Filling of the Gaussian LUMO DOS by unhindered n-doping at high concentrations has been suggested for explanation,[22] which basically equals the case of dopant saturation as assumed here. The slight deviations in the measured E_F values are only due to the experimental uncertainties of IPES from which the LUMO onset positions have been derived (cf. Supporting Information, Figure S11 and Table S4), however, not impacting the conclusions on the underlying physics. Nevertheless, appearing kinks in the measured $E_F(MR)$ correlations have been explained in a slightly different manner, which will be addressed in the following, taking also the p-doping results into account.

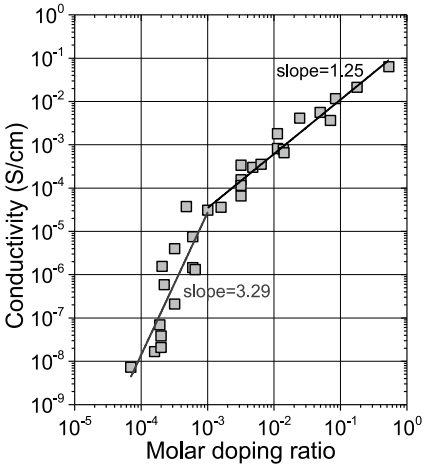

Figure 6. Conductivity of ZnPc:F_6-TCNNQ thin-films. Two regimes are identified with a transition at $MR \simeq 10^{-3}$. At lower concentrations, molecular doping is hindered by deep hole trap states.

2.4. Discussion

Kinks in Fermi level and conductivity versus free charge carrier density plots have recently been discussed in detail by Mehraeen et al. for the case of n-doping,[13,22] stating that they are both caused by the Fermi level crossing the transition energy between exponential tail states and Gaussian DOS, i.e., emerging at $E_F = E_\beta$ (cf. Equation (3)). In this context, kinks in corresponding conductivity plots are attributed to complete filling of the exponential tail states, regarded as electron traps, significantly reducing the effective carrier mobility at lower concentrations. Since we concluded dopant saturation and trap-filling regimes for all three investigated n-doped material systems, our results are not in direct contradiction to the conclusions drawn by Mehraeen et al., both approaches just differ in the type of the assumed electron trap states. However, considering the UPS and conductivity data of p-type doping presented here and in literature,[5,9,12,23,19] pinning of the Fermi level a few 100 meV above the HOMO onset at high doping concentrations cannot be consistently explained by the approach of Mehraeen et al. This circumstance becomes particularly clear by reviewing the UPS spectra of P5 and ZnPc in log-scale (cf. Supporting Information, Figures S9 and S10), where E_β values of 0.123 and 0.078 eV with respect to the HOMO onsets (E_{HOMO}) have been found. In contrast, kinks in the $E_F(MR)$ plots appear at 0.41 and 0.27 eV with respect to E_{HOMO}, i.e., much deeper within the gap, and are therefore regarded to $E_F = E_A$ rather than $E_F = E_\beta$. Furthermore, the conductivity versus MR plot of ZnPc:F_6-TCNNQ (Figure 6) does not show a kink at $MR \simeq 0.02$ as one would have expected from following the argumentation of Mehraeen et al. under consideration of the corresponding $E_F(MR)$ plot (Figure 3b). Thus, introduction of the acceptor level E_A is reasonable since it furthermore captures the experimentally observed incomplete dopant ionization at high concentrations in case of p-doping (reserve regime).

Finally, the appearance of the acceptor level E_A, so far just statistically motivated, should be justified on a microscopic level, which is sketched in Figure 4b. Due to doping acceptor type molecules into a host material either direct electron transfer from dopant to host (left) or host–dopant hybridization (right) might occur, depending on the mutual orientation and thus molecular orbital overlap of two adjacent host and dopant molecules. In the latter case, the hybrid antibonding state is supposed to appear a few 100 meV above the host HOMO level and to govern the actual doping process,[16,24] which is consistent with the conclusions drawn here. In particular, the transition from impurity saturation to reserve would correspond to Fermi level crossing the hybrid antibonding state, represented statistically by the acceptor level E_A. Increasing ionization potential values of the P_5:$C_{60}F_{36}$ thin-films from 4.88 eV at $MR = 2 \times 10^{-5}$

© 2015 WILEY-VCH Verlag GmbH & Co. KGaA, Weinheim

up to 5.33 eV at $MR = 0.33$ as well as appearing gap states in case of all n-doped films (cf. Supporting Information, Figures S6 and S8) furthermore indicate the formation of respective hybrids.

In case of direct charge transfer, justifying the appearance of E_A on a microscopic scale is less evident, however, recently we gave an explanation based on the formation of a common Fermi level for dopant and host molecules within a mixed film.[19] Here, the acceptor LUMO is pushed above the host HOMO upon occupation with electrons accompanied by an alignment of the individual dopant and host Fermi levels (cf. Figure 4b, left). The statistical acceptor depth E_A thus corresponds to an equilibrium activation energy between the host HOMO and the above lying dopant LUMO. Besides, doping induced gap states due to Coulomb interactions between ionized dopants and free carriers have been suggested.[25–27]

3. Conclusion

In conclusion, the Fermi level control by several orders of magnitude in various p- and n-doped organic semiconductor thin-films allowed us to study the mechanism of molecular doping over an extensive range. For the first time we can clearly reveal the regimes of trap-limitation, dopant saturation, and reserve. In particular, introduction of an acceptor level E_A, describing the amount of ionized dopants, marks the transition from dopant saturation to reserve for p-type doping, whereas 100% dopant ionization is found in case of n-doping even at very high concentrations. Our results show that it is possible to properly describe the corresponding properties of molecular doping by a classical statistical approach, which explains commonly observed low p-doping efficiencies, additionally extends the ideas of previously published modeling,[22] and gives evidence for the proposed underlying microscopic processes.[16] These findings are important on the roadmap toward cheap and flexible organic CMOS circuits, in particular, for the design of novel transistor concepts with reliable and precise parameter control.[28,29]

4. Experimental Section

Sample Preparation and UPS: The doped layers are thermally co-evaporated at room temperature under ultrahigh vacuum conditions (base pressure 1×10^{-9} mbar) by controlling the evaporation rates with two independent quartz crystal microbalances (QCMs). A sputter cleaned silver foil (99.995%, MaTecK, Juelich, Germany) is used as substrate. The host materials pentacene (Sensient, Wolfen, Germany) and zinc-phthalocyanine (CreaPhys, Dresden, Germany) were purified threefold by 3-zone vacuum gradient sublimation. The fullerene C_{60} has been purchased from CreaPhys of sublimed purity grade and is used as delivered. The dopant compounds $C_{60}F_{36}$ (MTR Ltd., USA), 1,3,4,5,7,8-hexafluorotetracyanonaphthoquinodimethane (F_6-TCNNQ) and 1,3,4,6,7,8-hexayhydro-2H-pyrimido[1,2-a]pyrimidine (W_2(hpp)$_4$) (both Novaled GmbH, Dresden, Germany) are used as delivered as well. The chemical structures are shown in Figure 1a. Doping ratios below 10^{-3} are achieved by evaporating the dopant molecules through a rotating shutter (2–3 Hz) positioned between the substrate and the QCM. The circular shutter is partly opened (≃18°) which reduces the effective molecule transmission to ≈5%. The functionality of this system has been verified by checking the actually achieved doping concentration with X-ray photoemission spectroscopy on a highly doped sample. In this article, we give the doping concentration as molar ratio, defined as the ratio of the number of dopant to host molecules per volume, i.e., $MR = N_A/N_0$. The UPS measurements are performed with a Phoibos 100 system (Specs, Berlin, Germany) under UHV conditions (base pressure 5×10^{-11} mbar). Sample transfer without breaking vacuum conditions is ensured by a direct connection of the UPS to the evaporation chamber. The energy resolution (HeI, 21.22 eV) is 130 meV and the experimental error (reproducibility) is estimated to 50 meV. During the UPS measurement the sample is set to an acceleration potential of −8 V. For each spectrum, the emission features due to secondary line excitations of the HeI discharge lamp are subtracted.[12] The measurements are kept as short as possible to avoid degradation of the organic materials and charging effects.

Numerical Calculations: The neutrality condition (Equation (1)) has been solved by numerical evaluation of the corresponding Fermi integral using the open source software GNU Octave running under Ubuntu. Here, an energy discretization in-between 0.001...0.005 eV is applied for stepwise integration and varying Fermi energies. The calculation parameters are summarized in Table S2 (p-doping) and Table S3 (n-doping) of the Supporting Information.

Supporting Information

Supporting Information is available from the Wiley Online Library or from the author.

Acknowledgements

The research was funded by the Deutsche Forschungsgemeinschaft and the US National Science Foundation within the joint project "MatWorldNet" (Project Code LE 747/44–1) as well as by the King Abdullah University of Science and Technology. Furthermore, the authors thank Novaled GmbH (Dresden, Germany) for providing the dopant materials as well as Selina Olthof for fruitful discussions and providing the IPES data.

Received: December 23, 2014
Revised: January 31, 2015
Published online: March 26, 2015

[1] S. M. Sze, *Physics of Semiconductor Devices*, 3rd ed., John Wiley and Sons, New York **1981**.
[2] K. Walzer, B. Männig, M. Pfeiffer, K. Leo, *Chem. Rev.* **2007**, *107*, 1233.
[3] B. Lüssem, M. Riede, K. Leo, *Phys. Status Solidi A* **2013**, *210*, 9.
[4] P. Pingel, R. Schwarzl, D. Neher, *Appl. Phys. Lett.* **2012**, *100*, 143303.
[5] S. Olthof, W. Tress, R. Meerheim, B. Lüssem, K. Leo, *J. Appl. Phys.* **2009**, *106*, 103711.
[6] C. K. Chan, E.-G. Kim, J.-L. Bredas, A. Kahn, *Adv. Funct. Mater.* **2006**, *16*, 831.
[7] S. P. Tiwari, W. J. Potscavage, T. Sajoto, S. Barlow, S. R. Marder, B. Kippelen, *Org. Electron.* **2010**, *11*, 860.
[8] J.-H. Lee, H.-M. Kim, K.-B. Kim, J.-J. Kim, *Org. Electron.* **2011**, *12*, 950.
[9] M. Kröger, S. Hamwi, J. Meyer, T. Riedl, W. Kowalsky, A. Kahn, *Org. Electron.* **2009**, *10*, 932.
[10] T. Glaser, S. Beck, B. Lunkenheimer, D. Donhauser, A. Köhn, M. Kröger, A. Pucci, *Org. Electron.* **2013**, *14*, 575.
[11] S. Hamwi, J. Meyer, T. Winkler, T. Riedl, W. Kowalsky, *Appl. Phys. Lett.* **2009**, *94*, 253307.

© 2015 WILEY-VCH Verlag GmbH & Co. KGaA, Weinheim

[12] M. L. Tietze, L. Burtone, M. Riede, B. Lüssem, K. Leo, *Phys. Rev. B* **2012**, *86*, 035320.
[13] S. Olthof, S. Mehraeen, S. K. Mohapatra, S. Barlow, V. Coropceanu, J.-L. Bredas, S. R. Marder, A. Kahn, *Phys. Rev. Lett.* **2012**, *109*, 176601.
[14] M. L. Tietze, K. Leo, B. Lüssem, *Org. Electron.* **2013**, *14*, 2348.
[15] A. Mityashin, Y. Olivier, T. Van Regemorter, C. Rolin, S. Verlaak, N. G. Martinelli, D. Beljonne, J. Cornil, J. Genoe, P. Heremans, *Adv. Mater.* **2012**, *24*, 1535.
[16] I. Salzmann, G. Heimel, S. Duhm, M. Oehzelt, P. Pingel, B. George, A. Schnegg, K. Lips, R.-P. Blum, A. Vollmer, N. Koch, *Phys. Rev. Lett.* **2012**, *108*, 035502.
[17] M. L. Tietze, W. Tress, S. Pfützner, C. Schünemann, L. Burtone, M. Riede, K. Vandewal, S. Olthof, P. Schulz, A. Kahn, K. Leo, *Phys. Rev. B* **2013**, *88*, 085119.
[18] P. Pahner, H. Kleemann, L. Burtone, M. L. Tietze, J. Fischer, K. Leo, B. Lüssem, *Phys. Rev. B* **2013**, *88*, 195205.
[19] M. L. Tietze, F. Wölzl, T. Menke, A. Fischer, M. Riede, K. Leo, B. Lüssem, *Phys. Status Solidi A* **2013**, *210*, 2188.
[20] J. Steiger, R. Schmechel, H. von Seggern, *Synth. Met.* **2002**, *129*, 1.
[21] P. Pahner, M. L. Tietze, B. Lüssem, K. Leo, unpublished.
[22] S. Mehraeen, V. Coropceanu, J.-L. Bredas, *Phys. Rev. B* **2013**, *87*, 195209.
[23] B. Männig, M. Pfeiffer, A. Nollau, X. Zhou, K. Leo, P. Simon, *Phys. Rev. B* **2001**, *64*, 195208.
[24] H. Mendez, G. Heimel, A. Opitz, K. Sauer, P. Barowski, M. Oehzelt, J. Soeda, T. Okamoto, J. Takeya, J.-B. Arlin, J.-Y. Balandier, Y. Geerts, N. Koch, I. Salzmann, *Angew. Chem.* **2013**, *125*, 7905.
[25] P. Pingel, D. Neher, *Phys. Rev. B* **2013**, *87*, 115209.
[26] V. Arkhipov, P. Heremans, E. Emelianova, H. Bässler, *Phys. Rev. B* **2005**, *71*, 045214.
[27] V. Arkhipov, E. Emelianova, P. Heremans, H. Bässler, *Phys. Rev. B* **2005**, *72*, 235202.
[28] B. Lüssem, M. L. Tietze, H. Kleemann, C. Hossbach, J. W. Bartha, A. Zakhidov, K. Leo, *Nat. Commun.* **2013**, *4*, 2775.
[29] H. Kleemann, A. A. Günther, K. Leo, B. Lüssem, *Small* **2013**, *9*, 3670.

© 2015 WILEY-VCH Verlag GmbH & Co. KGaA, Weinheim